THE JOURNAL OF PHYSICAL CHEMISTRY B
A JOURNAL OF THE AMERICAN CHEMICAL SOCIETY

pubs.acs.org/JPCB

Article

Water Dynamics in Aqueous Poly-*N*-Isopropylacrylamide Below and Through the Lower Critical Solution Temperature

Sean A. Roget, Kimberly A. Carter-Fenk, and Michael D. Fayer*

Cite This: *J. Phys. Chem. B* 2022, 126, 7066−7075

Read Online

ACCESS | Metrics & More | Article Recommendations | Supporting Information

ABSTRACT: Poly-*N*-isopropylacrylamide (PNIPAM) is a thermo-responsive polymer that exhibits a reversible structural change from extended chains to aggregates in aqueous solution above its lower critical solution temperature (LCST). Using polarization-selective IR pump−probe spectroscopy, the water orientational dynamics in PNIPAM from below to above the LCST were examined and compared to those of its monomer solution, *N*-isopropylacrylamide (NIPAM), polyacrylamide, and an acrylamide monomer solution, which are not thermo-responsive. The OD stretch of dilute HOD in H_2O is used as a vibrational probe of water orientational dynamics. Below the LCST of the polymer, NIPAM and PNIPAM solutions exhibited identical water dynamics that were significantly different from those of bulk water, containing both faster and slower components due to solute−water interactions. Therefore, there is no difference in the nature of water interactions with a single NIPAM moiety and a long polymer chain. For all systems, including PNIPAM below and above the LCST, the orientational dynamics were modeled with a bulk water component and a polymer/monomer-associated component based on previous experimental and computational findings. Above the LCST, PNIPAM showed fast water orientational relaxation but much slower long-time dynamics compared to those of NIPAM. The slow component in PNIPAM, which was too slow to be accurately measured due to the limited OD vibrational lifetime, is ascribed to water confined in small voids (<2 nm in diameter) of PNIPAM globules. These results highlight important details about thermo-responsive polymers and the dynamics of their solvation water as they undergo a significant structural change.

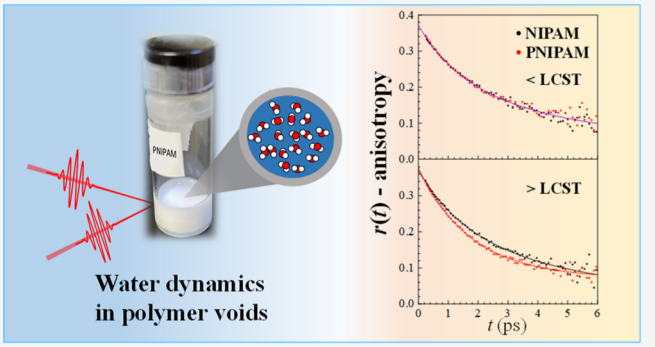

Downloaded via STANFORD UNIV on December 6, 2022 at 21:40:54 (UTC).
See https://pubs.acs.org/sharingguidelines for options on how to legitimately share published articles.

1. INTRODUCTION

Hydrogels are versatile materials with applications ranging from personal hygiene products and cosmetics to advanced biotechnologies such as bioactuators for artificial muscles or biosensors that can detect physiological, biochemical processes.[1−4] These materials are hydrophilic, cross-linked polymers that can retain large amounts of water. The physical properties can be fine-tuned based on the choice of the monomer and also through copolymerization of different monomers.[1] Smart polymers are a particular class of hydrogels that show responsiveness to stimuli such as pH, temperature, and humidity.[5,6] These external factors can affect the overall structure and properties of the material. Poly-*N*-isopropylacrylamide (PNIPAM) is a well-studied example of a thermo-responsive polymer.[7] The monomer structure is shown in Figure 1. As the polymer is heated above its lower critical solution temperature (LCST) of ∼32 °C, the material undergoes a phase transition from a water-swollen, extended polymer network to a collapsed state with polymer-rich domains.[8,9] This is known as the coil−globule transition, which refers to the conformations of the polymer structure below and above the LCST, respectively, and it has garnered interest from the scientific community, especially in the

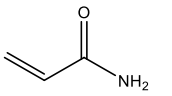

Acrylamide (AAm)

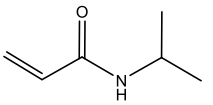

N-isopropylacrylamide (NIPAM)

Figure 1. Chemical structures of AAm and NIPAM monomers.

Received: August 2, 2022
Revised: August 11, 2022
Published: September 6, 2022

© 2022 American Chemical Society

https://doi.org/10.1021/acs.jpcb.2c05506
J. Phys. Chem. B 2022, 126, 7066−7075

biomedical field, because of its potential in a variety of applications including drug delivery and tissue engineering.[10,11]

Experimental and computational studies of the coil−globule transition of PNIPAM indicate that the phase transition is due to the thermodynamically favored entropy gain that arises when the polymer chains collapse.[12] It is widely accepted that, although it is enthalpically favorable to solvate the hydrophilic amide groups of the polymer, the hydration of the hydrophobic regions imparts order on the water molecules in the first solvation shell, which decreases the entropy.[13] Thus, as the temperature increases, it becomes less favorable to solvate the hydrophobic groups, resulting in the aggregation of the polymer chains to reduce exposure of the hydrophobic groups to water.

Various experimental techniques, including FT-IR,[14−17] Raman,[18] and terahertz[19] spectroscopy, have highlighted the importance of polymer−water and polymer−polymer interactions in the coil−globule transition. Most of the experimental studies have examined the phase transition from the perspective of the polymer chains. For example, experiments employing linear IR spectroscopy have been used to inspect structural changes through the amide I and II vibrational modes of PNIPAM and the *N*-isopropylacrylamide (NIPAM) monomer. Notably, it has been shown that there is partial dehydration of the hydrophilic amide groups through the LCST as well as the formation of intramolecular and intermolecular amide hydrogen bonds (H-bonds). In addition, experiments and MD simulations indicate that there is also dehydration of the hydrophobic moieties, which leads to a favorable entropy gain.[13,14,17,20] However, it is clear that water is critical to the underlying transition mechanism and plays a crucial role in thermo-responsive polymers and, more generally, hydrogel materials. The limited studies on the water structure and dynamics using techniques such as dielectric relaxation,[21,22] NMR,[23−25] and quasi-elastic neutron scattering[26,27] show a reduction in bound or hydrating water near the polymer through the LCST, which exhibits much slower dynamics than bulk water.

Linear and ultrafast nonlinear IR spectroscopy are techniques that can directly probe the structure and dynamics of water in complex aqueous systems using the OD stretch of dilute HOD. The properties of bulk water stem from its highly dynamic, approximately tetrahedral H-bond network, which is constantly rearranging on a picosecond timescale. Ultrafast IR studies have successfully examined time-resolved dynamics of water molecules near ions[28−31] and small organic molecules[32−34] as well as water confined within spherical reverse micelles (RMs),[35,36] lamellar structures,[37] and complex polymeric systems.[38−41] In general, nanoscale confinement or interactions with solutes perturbs the H-bond network structure and slows water H-bond dynamics.[35−42] Recent investigations of linear polyacrylamide (PAAm) and cross-linked hydrogels demonstrate the strong influence of polymer−water interactions on water H-bond dynamics.[40,41] The water within the hydrogels show much slower reorientation and spectral diffusion dynamics (structural evolution) than those of bulk water. The dynamics become slower with increasing polymer concentration, which coincides with a reduction in the average pore size of the hydrogels.[40,43,44] However, a comparison of the water dynamics within the PAAm hydrogels, the polymers, and the acrylamide (AAm) monomer solutions at different concentrations showed that the water dynamics were identical and primarily affected by interactions with the monomer units. The polymer structure, cross-linked or not, does not have an impact on the water dynamics compared to monomer solutions of the same concentration.

Here, we report the investigation of water reorientation in PNIPAM using ultrafast temperature-dependent polarization-selective pump−probe (PSPP) IR spectroscopy. Through the LCST, PNIPAM undergoes a significant structural change, which affects the polymer−water interactions and, therefore, the water dynamics in this system. To interpret the results, the water dynamics in PNIPAM were compared to those of the NIPAM monomer solution as well as PAAm and its monomer solution, which do not exhibit a coil−globule transition. Similar to previous results with PAAm, PNIPAM and NIPAM showed identical water reorientation dynamics at temperatures below the LCST. Above the LCST, differences in the water reorientation dynamics of PNIPAM were observed in comparison to those of NIPAM, implying that the water dynamics in the polymer system was affected by the coil−globule transition. By modeling the dynamics with a two-component model, as suggested from detailed MD simulations of AAm oligomer systems,[41] we rationalize how the changes in the dynamics of water interacting with PNIPAM above the LCST arise.

2. MATERIALS AND METHODS

2.1. Sample Preparation. AAm, NIPAM, ammonium persulfate (APS), and *N*,*N*,*N*′,*N*′-tetramethylethylenediamine (TEMED) were purchased from Sigma-Aldrich (purity ≥ 99%) and used as received. Monomer solutions of AAm and NIPAM were prepared at the 36:1 molar ratio (H_2O to monomer). For the IR experiments, the monomer solutions were prepared with 5% HOD in H_2O, by mole fraction, rather than neat water. A few drops of the monomer solution were sandwiched between two CaF_2 windows separated by a 12 μm Teflon spacer and housed in an aluminum sample cell. An airtight seal was created around the sample cell using melted paraffin wax to prevent any changes in the concentration of the solution through evaporation, which can readily occur when the sample is heated over the course of the nonlinear experiments.

PAAm and PNIPAM were prepared by adding 10 μL of 10% (w/v) APS solution (initiator) followed by 1 μL of TEMED (catalyst) to 1 mL of the corresponding monomer solution. Polymers were prepared without the addition of cross-linking agents. Immediately after mixing, the solution was prepared in a sample cell with the same path length as that of the monomer solutions. After 1 h, the solution was mostly polymerized, and paraffin wax was applied. The samples continued to polymerize for an additional 15 h before performing the nonlinear experiments. Preparing the samples in the sample cell improves their optical quality. Any changes in the sample over the course of preparation and experiments were monitored through Fourier transform infrared (FT-IR) spectroscopy. The LCST was observed at 32 °C (through the detection of scattered IR light), indicating that the preparation formed a polymer solution with a significant fraction of high-molecular weight PNIPAM chains.[45]

2.2. Vibrational Spectroscopy. Linear absorption spectra were collected using an FT-IR spectrometer with a resolution of 0.5 cm^{-1}. The sample compartment of the spectrometer was purged with atmospheric carbon dioxide and water. Monomer and polymer samples prepared with neat water and with 5%

https://doi.org/10.1021/acs.jpcb.2c05506
J. Phys. Chem. B 2022, 126, 7066−7075

HOD in H_2O were measured to isolate the OD stretch of HOD from background absorption features. Studying the OD stretch of HOD in solution rather than the OH stretch of H_2O eliminates vibrational excitation transfer.[46,47] In addition, the OD stretch of HOD is a local vibrational mode, which has been shown to be a good reporter of the H-bond structure and dynamics in various chemical systems. The OD stretch absorption is isolated from H_2O vibrational modes.

Nonlinear polarization-selective pump−probe (PSPP) experiments were performed using a laser system that has been previously described in detail.[48] Briefly, a Ti:Sapphire oscillator/regenerative amplifier system was used to pump an optical parametric amplifier at 2 kHz to generate mid-IR pulses that were centered at ∼4 μm and ∼65 fs in pulse duration. To perform the PSPP experiment, the mid-IR pulse was split into a strong pump pulse and a weaker probe pulse (90:10 in intensity) and crossed in the sample to generate a third-order, nonlinear signal. The signal was frequency-resolved with a monochromator configured as a spectrograph with a 32 pixel mercury cadmium telluride detector. The polarization of the pump pulse was set to +45° with respect to the probe pulse, which was horizontally polarized (0°). Immediately after the sample, the signal was resolved either parallel (+45°) or perpendicular (−45°) to the pump pulse and then finally resolved to 0°. By resolving the signal in this manner, any polarization bias from the diffraction grating in the spectrograph is eliminated. The time delay between the pump and probe pulse was controlled using a precision delay stage. By scanning the pump pulse relative to the probe pulse, the parallel and perpendicular signals, $S_{\parallel}(t)$ and $S_{\perp}(t)$, respectively, were acquired. The polarized signals can be used to calculate vibrational and orientational relaxation of the vibrational probe using the following equations

$$P(t) = S_{\parallel} + 2S_{\perp} \tag{1}$$

$$r(t) = \frac{S_{\parallel} - S_{\perp}}{S_{\parallel} + 2S_{\perp}} = 0.4C_2(t) \tag{2}$$

where $P(t)$ is the population relaxation of the probe molecule and $r(t)$ is the anisotropy, which is proportional to $C_2(t)$, the second-order Legendre polynomial orientational correlation function given by

$$C_2(t) = \langle P_2[\hat{\mu}(t)\cdot\hat{\mu}(0)]\rangle \tag{3}$$

where P_2 is the second-order Legendre polynomial, $\hat{\mu}$ is the transition dipole unit vector, and $\langle \ldots \rangle$ denotes an ensemble average. Vibrational relaxation of the excited OD stretch of HOD leads to a transient long-lived signal, which is a result of a slight temperature increase from the dissipation of the vibrational energy as heat. The heating signal was removed from the pump−probe signal using a well-documented procedure so that the vibrational and orientational relaxation can be accurately characterized.[49,50] Pump−probe experiments were averaged until a high signal-to-noise ratio was achieved for fitting the anisotropy decays (∼200 scans of each time point over the full time range). Representative polarized pump−probe decays and the heating signal determined from fits are shown in Figure S1 in the Supporting Information. Curve fitting was performed using the nonlinear curve fit tool in OriginPro 2018 software. Error in the fits were reported from the standard error output of the software or the standard deviation over three identical samples (reporting the larger of the two outputs). Anisotropy decays presented in this report correspond to the center frequency of the OD stretch mode in the various monomer solutions and aqueous polymers (2510 cm^{-1}). No notable frequency dependence in the orientational dynamics was observed.

For the temperature-dependent IR experiments, the sample cell was heated to the desired temperature using a cartridge heater connected to a temperature controller. Room-temperature experiments were performed at 23 °C and were conducted without heating.

3. RESULTS AND DISCUSSION

3.1. Linear Spectra. The linear absorption spectra of the OD stretch of HOD in bulk water, NIPAM, and PNIPAM at room temperature (23 °C) are presented in Figure 2. The

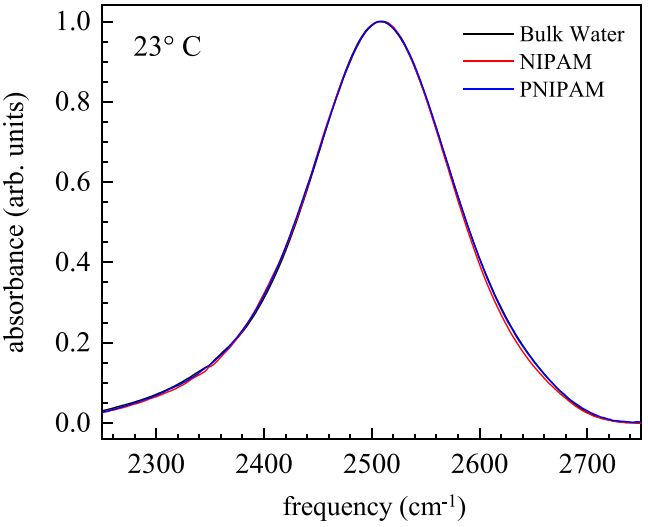

Figure 2. Normalized and background-subtracted linear absorption spectra of the OD stretch of dilute HOD in bulk water, NIPAM, and PNIPAM.

vibrational mode is significantly inhomogeneously broadened due to the water H-bond network, which has a wide variety of H-bonding configurations. In bulk water, the OD stretch is centered at 2509 cm^{-1} and has a FWHM of 159 cm^{-1}. The number and strength of the H-bonds of a given HOD molecule within the H-bond network determines the frequency of the vibrational transition. Stronger H-bonding and/or a greater number of H-bonds will lower the vibrational frequency of the OD stretch.

When dilute HOD is introduced into complex aqueous environments, such as in RMs or polyelectrolyte membranes, the shape and position of the OD stretch vibrational mode are altered because the water H-bond network is modified by interactions with solutes and interfaces.[51,52] In these particular examples, the OD stretch shifts to higher frequencies due to a distinct ensemble of water molecules near the interface, which are in weak H-bonding configurations. The OD stretch of HOD in NIPAM and PNIPAM (Figure 2) is indistinguishable from HOD in bulk water. This indicates that the polymer−water interactions are of similar strength to water−water interactions, likely due to the hydrophilic nature of the amide group. This is similar to previous observations of the linear spectra of HOD in PAAm (shown in Figure S2) and PAAm hydrogels.[40,41] However, in comparison to PAAm, PNIPAM

https://doi.org/10.1021/acs.jpcb.2c05506
J. Phys. Chem. B 2022, 126, 7066−7075

has a large hydrophobic isopropyl group in place of one of the H-bond donors of the amide moiety. This hydrophobic group is critical to the thermo-responsive nature of PNIPAM, and simulations have suggested that it leads to strong water−water H-bonding configurations in the first solvation shell of the isopropyl group.[13] However, the linear spectrum of HOD in PNIPAM is identical to the bulk water spectrum. Therefore, there is no evidence in the hydroxyl absorption spectrum of stronger water−water H-bonding interactions present in the system compared to those in pure water. However, significant changes in the dynamics of water are observed in PNIPAM.

3.2. Temperature-dependent Water Orientational Dynamics in AAm, PAAm, and NIPAM. The anisotropy was calculated from the polarized signals of the PSPP experiment as given by eq 2. It is proportional to the second-order Legendre polynomial orientational correlation function of the transition dipole moment, $C_2(t)$, which provides details on the orientational dynamics of the HOD probe. For the OD stretch vibrational mode of HOD, the transition dipole moment is essentially along the OD bond.[53] At $t = 0$, the anisotropy has a maximum value of 0.4 since the initial and final directions of the dipole (OD bond) vectors are perfectly correlated. The anisotropy decays to 0 after a sufficiently long time in an isotropic medium due to molecular reorientation.

The temperature dependence of water reorientation in AAm, PAAm, and NIPAM was examined to understand the water dynamics in the absence of the coil−globule transition present in PNIPAM at 32 °C. Anisotropy decays of HOD in bulk water, PAAm, PNIPAM, and their corresponding monomer solutions at 23 °C are shown in Figure 3. The experimental

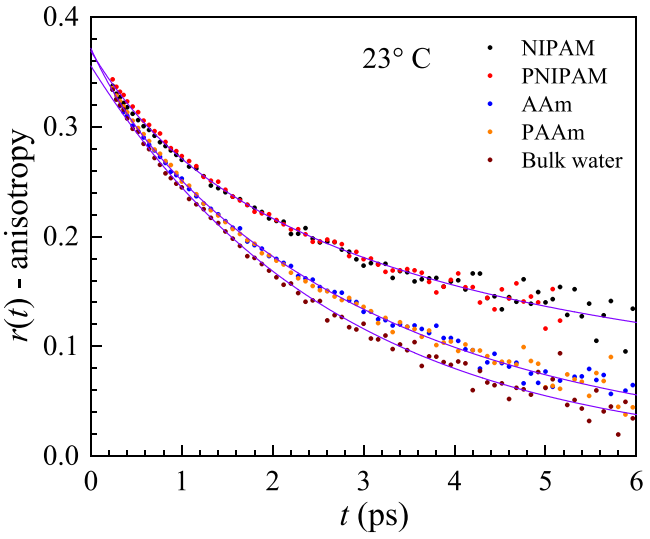

Figure 3. Anisotropy decays (points) and their corresponding fits (purple curves) of the OD stretch of HOD in bulk water, PAAm, PNIPAM solutions, and their respective monomer solutions at 23 °C.

decays begin at ∼240 fs as there is a strong non-resonant signal that occurs due to the time overlap of the pump and probe pulses, which extends past $t = 0$. When the fits of the decays are extrapolated to $t = 0$, it is observed that the decays begin below 0.4. The deviation from the theoretical initial value of the anisotropy is caused by ultrafast inertial motions that occur on a time scale <100 fs and is obscured from experimental observation because of the non-resonant signal.[54] The monomer/polymer systems show slower reorientation dynamics than bulk water following the inertial component, with NIPAM and PNIPAM displaying a more dramatic slowdown in comparison to AAm and PAAm. This is unlike the linear spectra in the previous section, which showed no change in the absorption spectrum due to the introduction of the monomers or polymers. As observed in previous PSPP experiments, which also included cross-linked PAAm hydrogels, AAm and PAAm have identical water dynamics within experimental errors.[41] Here, it is found to be true for NIPAM and PNIPAM below the LCST as well.

Anisotropy decays of HOD in AAm, PAAm, and NIPAM measured at 23, 32, and 37 °C are shown in Figure 4. As

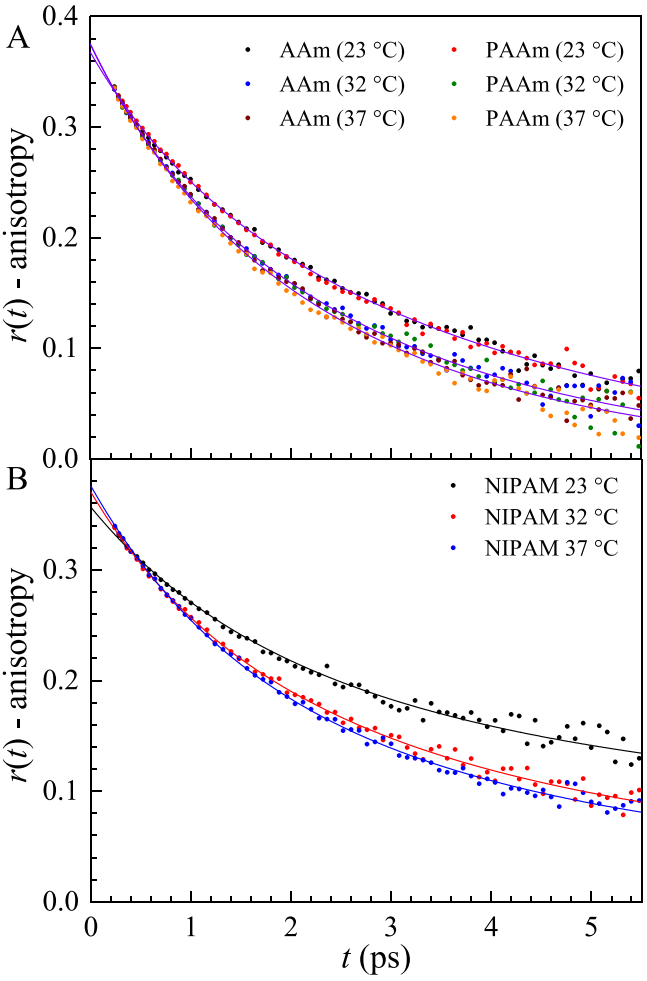

Figure 4. Anisotropy decays of the OD stretch of HOD in (A) AAm and PAAm and (B) NIPAM solutions (points) and fits (curves) to the two-component model at 23, 32, and 37 °C. At each temperature in (A), the polymer and monomers are the same within the experimental error.

temperature is increased, the water dynamics in AAm, NIPAM, and PAAm become faster; it is important to note that the dynamics in the AAm monomer solution and aqueous PAAm are the same at each temperature within errors. In bulk water, the reorientation of HOD is described well by a single-exponential decay with a time constant of 2.6 ps at room temperature.[28,50] As temperature increases, the dynamics become faster, with an observed activation energy of 18 ± 2 kJ/mol as shown in Figures S3 and S4 of the Supporting

https://doi.org/10.1021/acs.jpcb.2c05506
J. Phys. Chem. B 2022, 126, 7066−7075

Information in agreement with the literature.[55,56] The anisotropy decays for the monomer/polymer systems can be fit with a biexponential decay, implying there are two reorientation time scales.[41] MD simulations of water near AAm monomers and oligomers have shown that the overall water orientational dynamics in these systems over a range of concentrations can be described with three different dynamical water ensembles.[41] Water directly H-bonded to the amide group displayed the slowest dynamics in the simulated AAm systems, followed by water interacting with AAm but not H-bonded. Water outside the first solvation shell was found to have essentially bulk water dynamics at 36:1 molar ratio. Based on these results, it is reasonable to fit the anisotropy decays to a two-component model, noting that there is a negligible amount of water forming H-bonds with amide groups (2−3 hydroxyls) compared to the number of water molecules not H-bonded. The anisotropy can be described as follows

$$r(t) = 0.4[aC_{2,w}(t) + (1 - a)C_{2,m}(t)] \quad (4)$$

where a is the relative amplitude of the bulk water component and $C_{2,w}(t)$ and $C_{2,m}(t)$ are the orientational correlation functions for water associated with other water molecules and water associated with the moieties of the polymer or free monomers in solution (water in the first solvation shell of the polymer or monomer), respectively.

$C_{2,w}(t)$ is the bulk water correlation function, which is a single-exponential decay with temperature dependence that can be measured independently (Figures S3 and S4). Simulations of PNIPAM (below the LCST), PAAm, and their respective monomers in solution show that these systems have a significant component of bulk water and a component of water associated (first solvation shell) with the polymers/monomers.[41,57] If $C_{2,m}(t)$ was also a single-exponential decay, the two-component model (eq 4) would be a biexponential decay with time constants being summarized in Table S2 for the polymer/monomer systems. However, these time constants are either too fast (∼0.8 to 1.8 ps) or too slow (∼4 to 10 ps) to correspond to bulk water. Therefore, $C_{2,m}(t)$ is taken to be a biexponential decay and the two-component model is effectively a triexponential decay that includes the fraction of bulk water from simulations and the bulk water orientational dynamics.

Biexponential orientational relaxation dynamics are typically observed in aqueous systems in which water interacts with species other than water molecules.[30,58−60] These dynamics can be described using the wobbling-in-a-cone model.[61−63] The faster time scale occurs due to restricted, diffusive orientational motions within a cone of a half angle, θ_c. The slower time constant describes the complete orientational relaxation, following the release of the constraints that restrict the angular motions at short time. Water associated with a polymer/monomer can wobble through some angular range, prior to complete orientation relaxation. From the wobbling model, $C_{2,m}(t)$ is described as follows

$$C_{2,m}(t) = r_e(0)[S_2^2 + (1 - S_2^2)\exp(-t/t_c)]\exp(-t/t_m) \quad (5)$$

where $r_e(0)$ is the decay extrapolated to $t = 0$ that accounts for inertial reorientation.[64] S_2 is the generalized order parameter for the diffusive wobbling motion, t_c is the restricted angular diffusion time constant, and t_m is the complete angular diffusion time constant. S_2 is related to the wobbling cone angle, θ_c, using the following expression

$$S_2 = \frac{1}{2}\cos(\theta_c)[1 + \cos(\theta_c)] \quad (6)$$

The number of parameters in the two-component model is reduced by using the bulk water orientational relaxation time and the value of a obtained from an MD simulation study that quantified the number of water molecules in the first solvation shell of both PAAm and PNIPAM chains.[57] In the experiments, the concentrations of the solutions were 36 waters per monomer unit. From the simulation study, this results in ∼61 and ∼47% water molecules outside of the first solvation shell of PAAm and PNIPAM (a = 0.61 and 0.47), respectively. The value of $r_e(0)$ is known for bulk water as a function of temperature from Figure S3 and from the literature.[54] The observed value of $r_e(0)$, the experimental curve at $t = 0$, is the weighted sum of the water $r_e(0)$ and the $r_e(0)$ value for $C_{2,m}(t)$.

Fits to the anisotropy decays using the two-component model (triexponential) are shown in Figure 4 for PAAm and AAm (A) and for NIPAM (B) at 23, 32, and 37 °C. Fitting parameters for the anisotropy decays are shown in Table 1.

Table 1. Fit Parameters of $C_{2,m}(t)$ in PAAm and NIPAM (36 Waters per Monomer) Near the Center Frequency Using the Two Component Model

sample	a	t_1 (ps)	t_c (ps)[a]	θ_c (deg.)	$t_2 = t_m$ (ps)
bulk water					2.6 ± 0.1
PAAm 23 °C[b]	0.61	0.5 ± 0.2	0.6 ± 0.2	23 ± 3	5.1 ± 0.2
PAAm 32 °C[b]	0.61	0.6 ± 0.2	0.7 ± 0.2	24 ± 3	3.7 ± 0.2
PAAm 37 °C[b]	0.61	0.4 ± 0.2	0.5 ± 0.2	18 ± 3	3.3 ± 0.2
NIPAM 23 °C[c]	0.47	0.8 ± 0.2	0.9 ± 0.3	25 ± 3	19 ± 4
NIPAM 30 °C[c]	0.47	1.2 ± 0.2	1.3 ± 0.3	28 ± 3	13 ± 5
NIPAM 32 °C	0.47	1.0 ± 0.2	1.1 ± 0.3	26 ± 3	9 ± 2
NIPAM 34 °C	0.47	1.1 ± 0.2	1.3 ± 0.3	23 ± 3	8 ± 2
NIPAM 37 °C	0.47	1.1 ± 0.2	1.3 ± 0.3	27 ± 3	8 ± 2

[a] $t_c = (1/t_1 - 1/t_2)^{-1}$ where t_1 and t_2 are time constants from the biexponential fits to $C_{2,m}(t)$. [b] Simultaneous fit with anisotropy of water in AAm at given T. [c] Simultaneous fit with anisotropy of water in PNIPAM at given T.

The wobbling time constant, t_c, is longer in NIPAM than AAm/PAAm and the wobbling cone angle is much larger, indicating that water has more angular freedom at early time when interacting with the polymer with a bulky hydrophobic group. The results show that the monomer-associated free diffusion dynamics (t_m) in NIPAM solutions are three to four times slower than those in AAm/PAAm at all temperatures. This demonstrates that the additional isopropyl group of the NIPAM monomer unit has a significant effect on the NIPAM-associated water dynamics.

The mechanism for water reorientation in the bulk liquid, known as jump diffusion, is a concerted process that rearranges the H-bond network through breaking and making of H-bonds.[65] In jump diffusion, a water molecule must undergo a large angular jump (∼60°) to switch H-bonding configurations with its partners. The H-bond rearrangement, which randomizes water orientation, is a concerted process. It is highly dependent on the availability of H-bond acceptors outside of its first solvation shell. For this reason, reorientation of HOD in the H-bond network relies on cooperative rearrangements of

https://doi.org/10.1021/acs.jpcb.2c05506
J. Phys. Chem. B 2022, 126, 7066−7075

surrounding water molecules. It has been shown that in spite of the presence of solutes, jump diffusion is still the mechanism for water orientational relaxation.[66−68] However, it does result in the slowing of water dynamics by limiting the number of nearby H-bond acceptors available for H-bond rearrangements. This is an entropic factor shown by MD simulations using the excluded volume model.[66−68] When the solute has H-bond acceptor sites, the strength of the H-bond between the water H-bond donor and the solute molecule also plays a role in determining the water reorientation time scale.[67,68] Since the number of H-bond acceptor sites is unchanged between NIPAM and AAm, it is clear that the presence of the hydrophobic isopropyl group severely limits the number of potential H-bonding partners for water molecules in the first solvation shell, resulting in much slower dynamics near NIPAM monomers.

Previously, it was observed that AAm and PAAm (as well as cross-linked PAAm hydrogels) have identical water orientational dynamics (and structural dynamics), even at much higher concentrations. These results demonstrated that, for the same number of AAm moieties, there were no detectable changes in the water dynamics when the AAm monomers were free in solution or existed as a linear polymer or cross-linked hydrogel.[41] The dominant effect on the orientational dynamics is the interactions between the monomer units and water. This remains true for AAm/PAAm as temperature increases as shown in Figure 4. The interactions between water and NIPAM monomer in solution have a larger impact on the water dynamics than those of AAm. As shown in Figure 3, the water dynamics in NIPAM and PNIPAM are identical. This supports the previous observations that the water interactions with individual monomer moieties control the water dynamics. However, as we will show in the following section, the polymer organization of PNIPAM has a notable effect on the water dynamics as it goes through the coil−globule transition.

3.3. Temperature-Dependent Water Orientational Dynamics in PNIPAM. The anisotropy of HOD in NIPAM and PNIPAM at 30 and 34 °C, which are below and above the LCST of the polymer, is displayed in Figure 5. As observed at room temperature (Figure 3, 23 °C), the water orientational dynamics of the monomer and the polymer solutions are identical within error just below the LCST (Figure 5A). However, above the LCST, the water dynamics of the polymer and monomer solutions are no longer the same (Figure 5B).

Water reorientation in PNIPAM above the LCST can be fit with the two-component model as described in the previous section but with a modified physical interpretation. Below the LCST, there are two water ensembles, bulk water and water associated with the NIPAM monomer units of the polymer. The water dynamics are identical for NIPAM and PNIPAM below the LCST, showing that the dynamics of the associated water only depends on the interactions of water with the monomer units and bulk water beyond the first solvation shell. Above the LCST, there is substantial polymer aggregation. Inside the aggregates, there are voids ranging in size from large to very small. As discussed below, large voids will have cores of bulk water, and the associated water time constants should be similar to those below the phase transition. However, for smaller voids, the core water will have dynamics that are slower than those of bulk water, and the associated water dynamics are expected to also be slowed. For very small voids, <∼2 nm, both water associated with the polymer surface and water not

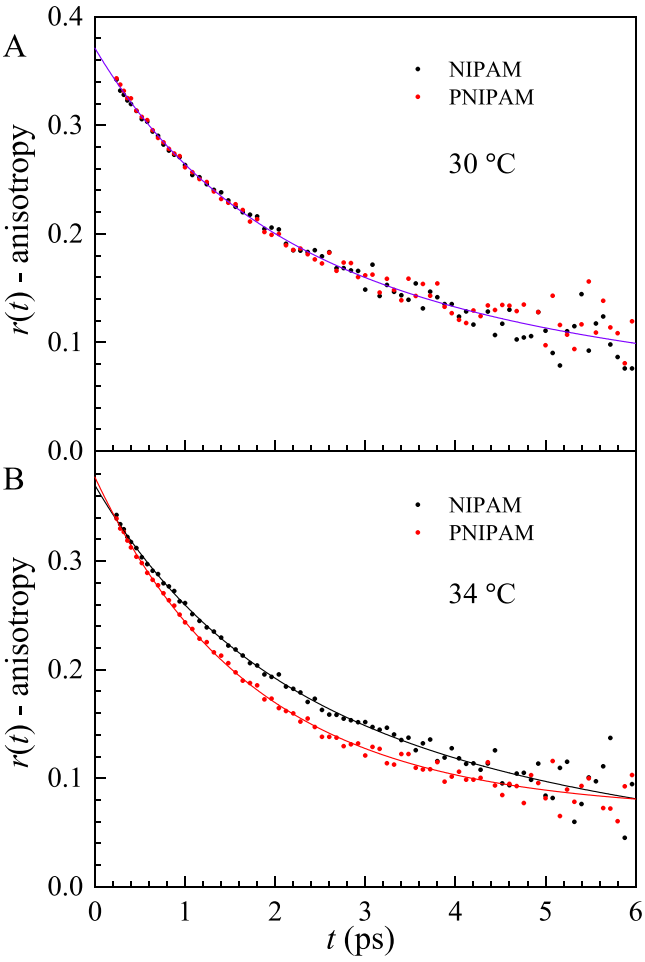

Figure 5. Anisotropy decays of the OD stretch of HOD in NIPAM and PNIPAM solutions (points) at (A) 30 °C and (B) 34 °C and fits (curves) to the two-component model.

in direct contact with the polymer will have exceedingly slow single-ensemble dynamics.

The experimental measurements observe bulk water and polymer-associated water dynamics as well as an average over all of the slower dynamics. The average will depend on the distribution of globule void sizes and shapes and how those sizes and shapes influence the water dynamics. Therefore, in using the two-component model to fit the anisotropy decays, the time constants in $C_{2,m}(t)$ are taken to reflect averages over the distribution of void sizes that produce dynamics that are not bulk-like.

Water reorientation in PNIPAM above the LCST was fit with the two-component model as described above (Figure 5B), and the results are compared to the water dynamics in the NIPAM solution in Table 2. In PNIPAM, water displays a similar restricted angular diffusion time constant as in the monomer solution, but the wobbling cone angle is much larger. This corresponds to the significant decay of the anisotropy of water in PNIPAM observed at early time in Figure 5B compared to that in the NIPAM solution. The free diffusion time constant of $C_{2,m}(t)$ in PNIPAM is significantly longer, much longer than can be precisely measured due to the limited vibrational lifetime of the OD stretch of the HOD probe (1.8 ps). The long time constant is consistent with the picture given above in which there is a distribution of voids, some of which are small enough to slow the dynamics substantially.

https://doi.org/10.1021/acs.jpcb.2c05506
J. Phys. Chem. B 2022, 126, 7066−7075

Table 2. Fit Parameters of $C_{2,m}(t)$ in NIPAM and PNIPAM (36 Waters per Monomer) Near the Center Frequency Using the Two-Component Model

sample	a	t_1 (ps)	t_c (ps)	θ_c (deg.)	$t_2 = t_m$ (ps)
NIPAM/PNIPAM 30 °C	0.47	1.2 ± 0.2	1.3 ± 0.3	28 ± 3	13 ± 5
NIPAM 34 °C	0.47	1.1 ± 0.2	1.3 ± 0.3	23 ± 3	8 ± 2
PNIPAM 34 °C	0.47	1.4 ± 0.1	1.4 ± 0.1	46 ± 2	-[a]
PNIPAM 34 °C	0.7	1.0 ± 0.3	1.0 ± 0.3	35 ± 3	-[a]

[a]Too long to be accurately determined.

Through the coil−globule transition, experiments and MD simulations indicate that there is a significant redistribution of polymer−water and polymer−polymer interactions due to the conformational change. In the globular conformation, the polymer forms hydrophobic aggregates as well as amide−amide H-bonding. Experimental investigations of the amide I and II bands suggest that as much as 26 and 50% of the amide acceptor sites and donor sites, respectively, become dehydrated and form NIPAM−NIPAM H-bonding interactions.[14,17] Furthermore, MD simulations suggest that the water within the first solvation shell of the isopropyl groups is reduced by as much as ∼30% when heated above the LCST due to hydrophobic aggregation.[13,69] Dehydration of the hydrophobic groups has been experimentally implied by the shifting of CH stretch modes as the temperature increases.[14,17] As discussed above, the slow dynamics observed here are likely a result of confinement effects in the polymer-rich domains. These dynamics have similar time scales to those of water in the confined nanopools of small RMs (<2 nm in diameter).[35] Confinement in RMs <2 nm in size affects all water molecules in the spherical hydrophilic domain, resulting in wobbling-in-a-cone dynamics with complete reorientation occurring in >100 ps. Although water is not confined in uniform spherical domains in the polymer globules, a comparison of the water dynamics to those in RMs sets the length scale of confinement.[35,37,42] This is because a spherical morphology results in confinement in all three dimensions, whereas a cylindrical channel or a lamellar structure has lesser degrees of confinement for similar length scales. For example, ultrafast IR experiments and simulations showed that bulk water dynamics still occur in the centers of cylindrical channels of mesoporous silica that are 2.4 nm in diameter.[42] Water in the polymer above the phase transition will be confined in three dimensions, indicating that water confined to voids of length scales of ≤ ∼2 nm will have very slow dynamics. Water in voids with diameters approximately 2 to 4 nm will have dynamics slower than bulk water dynamics but not extremely slow as in the voids that are ≤2 nm. Regions >4 nm will have bulk water dynamics away from the polymer surface.

Although the long time scale of the confined water in PNIPAM is similar to that of very small RMs, the cone angle observed here for PNIPAM is much larger than that of RMs and the monomer and polymer below the phase transition as shown in Table 2. The fit to the anisotropy decay in Figure 5B assumes that the number of polymer−water interactions, and therefore water−water interactions, has been maintained after the phase transition. However, the dehydration of PNIPAM that occurs when forming the polymer globules implies that there should be an increase in water−water interactions, and therefore, the relative amplitude of the bulk water component used for fitting should also be increased. By increasing the relative amplitude of the bulk water component, good fits to the anisotropy can be obtained with a decreased wobbling cone angle. In Figure 6, this is demonstrated by comparing the fits to the anisotropy with a = 0.47 and a = 0.7. The fits are

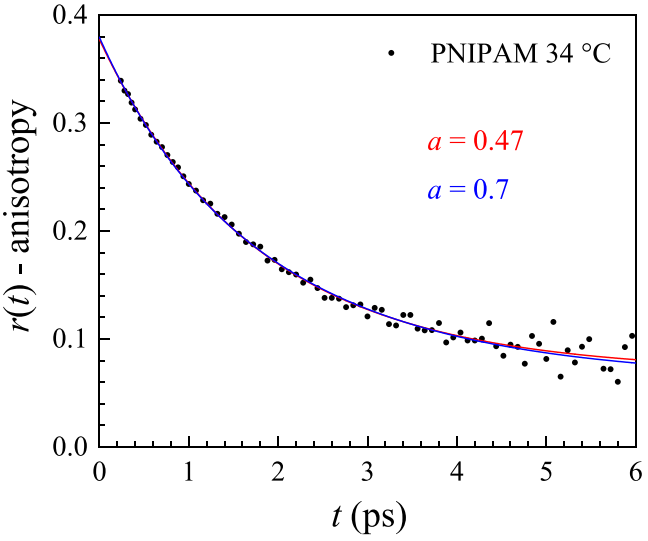

Figure 6. Anisotropy decay of the OD stretch of HOD in PNIPAM at 34 °C (points) and fits to the two-component model with the relative bulk water component being fixed at a = 0.47 (red curve) and a = 0.7 (blue curve).

virtually identical and result in a decrease in the cone angle from 46 to 35°, which approaches the results of water dynamics in both the RMs and the NIPAM monomer solution. Increasing the fraction of bulk water and the concomitant reduction in the cone angle to a more physically reasonable value are consistent with the dehydration of the polymers.

4. CONCLUDING REMARKS

We investigated the dynamics of water through the coil−globule transition of the thermo-responsive polymer, PNIPAM, using ultrafast temperature-dependent PSPP experiments on the OD stretch of dilute HOD present in the aqueous polymer system. We also explicated the influences on water dynamics of aqueous polymers and the monomers that comprise them. Above the LCST, the polymer undergoes dramatic changes in conformation, which are caused by competing solvation thermodynamics of the hydrophobic and hydrophilic functional groups of the polymer. Structure and dynamics of the surrounding water play critical roles in the phase behavior of PNIPAM. Water orientational dynamics in PNIPAM above and below the LCST were compared to those of PAAm and the corresponding monomer solutions to highlight dynamical changes that occur through the coil−globule transition.

The linear spectrum of the OD stretch of HOD in PNIPAM at room temperature, which is sensitive to the structure and

https://doi.org/10.1021/acs.jpcb.2c05506
J. Phys. Chem. B 2022, 126, 7066−7075

strength of the H-bond network, is the same as that of bulk water. This implied that the basic nature of the water H-bond network is not substantially impacted by the presence of the polymer and its bulky hydrophobic isopropyl group. Specifically, no obvious strengthening or ordering of the H-bond network is evident in the water spectrum. Although the H-bond network as reported by the linear spectrum remains bulk-like, aspects of the water reorientation dynamics in PNIPAM are substantially different compared to those of bulk water and PAAm at the concentration studied. As informed by previous MD simulations of AAm oligomers in solution, we modeled the temperature-dependent water reorientation dynamics of PAAm, PNIPAM, and their corresponding monomer solutions with a two-component model, with a bulk water component and a component for water associated with the polymer/monomer. The fraction of the bulk water component was fixed in the analysis based on MD simulations of solutions of PAAm and PNIPAM. Using this model, good agreement with MD simulations was obtained for the monomer/polymer-associated water dynamics in AAm and PAAm at room temperature, validating the choice of the relative amplitudes.[41,57] The monomer-associated water dynamics in NIPAM were up to four times slower at all temperatures than those of AAm and PAAm. These slow dynamics were rationalized through the excluded-volume effect.[68] This effect results from the presence of the hydrophobic isopropyl group on NIPAM that significantly reduces the availability of water H-bonding partners that are required for the concerted water reorientation process.

Although the water orientational dynamics of AAm and PAAm remained identical as the temperature increased, those of NIPAM and PNIPAM showed a marked change above the LCST of PNIPAM. The longest time constant for the polymer-associated water reorientation in PNIPAM slowed significantly and was similar to the dynamics of water in small RMs. In contrast to monodispersed RMs, water in the globular form of PNIPAM will exist in environments that have a broad range of sizes, from large bulk water regions to very small voids, which vastly slow water dynamics. The longest time constant in the fits to the PNIPAM water reorientation above the LCST reflects an average over time scales associated with the distribution of environments. There was also some evidence that the relative amplitude of the bulk water component increased, in agreement with experimental and MD simulations that show that the polymer becomes partially dehydrated past the LCST.

In summary, the presented water orientational dynamics within PNIPAM provides insight into the nature of water affected by the polymer in its two conformational phases. Understanding the dynamics and structure of water in PNIPAM is important for the development of thermo-responsive materials and, more generally, hydrogel materials. It also provides basic knowledge on how biological water can be affected by the conformations of large biomolecules. The time-resolved experimental information of the water dynamics presented here will greatly aid in future MD simulations of the solvation dynamics in complex macromolecular systems.

■ ASSOCIATED CONTENT

Supporting Information

The Supporting Information is available free of charge at https://pubs.acs.org/doi/10.1021/acs.jpcb.2c05506.

Representative polarized pump−probe decays, linear spectra of AAm and PAAm, temperature-dependent anisotropy decays of HOD in bulk water, Arrhenius plots of bulk water reorientation time constants, table of bulk water fit parameters for the anisotropy decays, and table of biexponential fit parameters for the anisotropy decays in the monomer/polymer systems (PDF)

■ AUTHOR INFORMATION

Corresponding Author

Michael D. Fayer − *Department of Chemistry, Stanford University, Stanford, California 94305, United States;* orcid.org/0000-0002-0021-1815; Phone: (650) 723-4446; Email: fayer@stanford.edu

Authors

Sean A. Roget − *Department of Chemistry, Stanford University, Stanford, California 94305, United States;* orcid.org/0000-0003-2470-3571

Kimberly A. Carter-Fenk − *Department of Chemistry, Stanford University, Stanford, California 94305, United States;* orcid.org/0000-0003-0071-7127

Complete contact information is available at: https://pubs.acs.org/10.1021/acs.jpcb.2c05506

Notes

The authors declare no competing financial interest.

■ ACKNOWLEDGMENTS

This work was funded by the Division of Chemical Sciences, Geosciences, and Biosciences, Office of Basic Energy Sciences of the U.S. Department of Energy, through grant no. DE-FG03-84ER13251.

■ REFERENCES

(1) Ahmed, E. M. Hydrogel: Preparation, characterization, and applications: A review. *J. Adv. Res.* **2015**, *6*, 105−121.

(2) Tavakoli, J.; Tang, Y. Hydrogel Based Sensors for Biomedical Applications: An Updated Review. *Polymers* **2017**, *9*, 364.

(3) Acome, E.; Mitchell, S. K.; Morrissey, T. G.; Emmett, M. B.; Benjamin, C.; King, M.; Radakovitz, M.; Keplinger, C. Hydraulically amplified self-healing electrostatic actuators with muscle-like performance. *Science* **2018**, *359*, 61.

(4) Shi, Q.; Liu, H.; Tang, D.; Li, Y.; Li, X.; Xu, F. Bioactuators based on stimulus-responsive hydrogels and their emerging biomedical applications. *NPG Asia Mater.* **2019**, *11*, 64.

(5) Koetting, M. C.; Peters, J. T.; Steichen, S. D.; Peppas, N. A. Stimulus-responsive hydrogels: Theory, modern advances, and applications. *Mater. Sci. Eng. R Rep.* **2015**, *93*, 1−49.

(6) Wei, M.; Gao, Y.; Li, X.; Serpe, M. J. Stimuli-responsive polymers and their applications. *Polym. Chem.* **2017**, *8*, 127−143.

(7) Heskins, M.; Guillet, J. E. Solution Properties of Poly(N-isopropylacrylamide). *J. Macromol. Sci., Chem.* **1968**, *2*, 1441−1455.

(8) Ito, D.; Kubota, K. Solution Properties and Thermal Behavior of Poly(N-n-propylacrylamide) in Water. *Macromolecules* **1997**, *30*, 7828−7834.

(9) Wu, C.; Wang, X. Globule-to-Coil Transition of a Single Homopolymer Chain in Solution. *Phys. Rev. Lett.* **1998**, *80*, 4092−4094.

(10) Lanzalaco, S.; Armelin, E. Poly(N-isopropylacrylamide) and Copolymers: A Review on Recent Progresses in Biomedical Applications. *Gels* **2017**, *3*, 36.

(11) Doberenz, F.; Zeng, K.; Willems, C.; Zhang, K.; Groth, T. Thermoresponsive polymers and their biomedical application in tissue engineering—a review. *J. Mater. Chem. B* **2020**, *8*, 607−628.

(12) Schild, H. G. Poly(N-isopropylacrylamide): experiment, theory and application. *Prog. Polym. Sci.* **1992**, *17*, 163−249.
(13) Deshmukh, S. A.; Sankaranarayanan, S. K. R. S.; Suthar, K.; Mancini, D. C. Role of Solvation Dynamics and Local Ordering of Water in Inducing Conformational Transitions in Poly(N-isopropylacrylamide) Oligomers through the LCST. *J. Phys. Chem. B* **2012**, *116*, 2651−2663.
(14) Maeda, Y.; Higuchi, T.; Ikeda, I. Change in Hydration State during the Coil−Globule Transition of Aqueous Solutions of Poly(N-isopropylacrylamide) as Evidenced by FTIR Spectroscopy. *Langmuir* **2000**, *16*, 7503−7509.
(15) Geukens, B.; Meersman, F.; Nies, E. Phase Behavior of N-(Isopropyl)propionamide in Aqueous Solution and Changes in Hydration Observed by FTIR Spectroscopy. *J. Phys. Chem. B* **2008**, *112*, 4474−4477.
(16) Lai, H.; Wu, P. A infrared spectroscopic study on the mechanism of temperature-induced phase transition of concentrated aqueous solutions of poly(N-isopropylacrylamide) and N-isopropylpropionamide. *Polymer* **2010**, *51*, 1404−1412.
(17) Futscher, M. H.; Philipp, M.; Müller-Buschbaum, P.; Schulte, A. The Role of Backbone Hydration of Poly(N-isopropyl acrylamide) Across the Volume Phase Transition Compared to its Monomer. *Sci. Rep.* **2017**, *7*, 17012.
(18) Ahmed, Z.; Gooding, E. A.; Pimenov, K. V.; Wang, L.; Asher, S. A. UV Resonance Raman Determination of Molecular Mechanism of Poly(N-isopropylacrylamide) Volume Phase Transition. *J. Phys. Chem. B* **2009**, *113*, 4248−4256.
(19) Shiraga, K.; Naito, H.; Suzuki, T.; Kondo, N.; Ogawa, Y. Hydration and Hydrogen Bond Network of Water during the Coil-to-Globule Transition in Poly(N-isopropylacrylamide) Aqueous Solution at Cloud Point Temperature. *J. Phys. Chem. B* **2015**, *119*, 5576−5587.
(20) Abbott, L. J.; Tucker, A. K.; Stevens, M. J. Single Chain Structure of a Poly(N-isopropylacrylamide) Surfactant in Water. *J. Phys. Chem. B* **2015**, *119*, 3837−3845.
(21) Füllbrandt, M.; Ermilova, E.; Asadujjaman, A.; Hölzel, R.; Bier, F. F.; von Klitzing, R.; Schönhals, A. Dynamics of Linear Poly(N-isopropylacrylamide) in Water around the Phase Transition Investigated by Dielectric Relaxation Spectroscopy. *J. Phys. Chem. B* **2014**, *118*, 3750−3759.
(22) Vijayakumar, B.; Takatsuka, M.; Kita, R.; Shinyashiki, N.; Yagihara, S.; Rathinasabapathy, S. Dynamics of the Poly(N-Isopropylacrylamide) Microgel Aqueous Suspension Investigated by Dielectric Relaxation Spectroscopy. *Macromolecules* **2022**, *55*, 1218−1229.
(23) Sierra-Martín, B.; Romero-Cano, M. S.; Cosgrove, T.; Vincent, B.; Fernández-Barbero, A. Solvent relaxation of swelling PNIPAM microgels by NMR. *Colloids Surf., A* **2005**, *270−271*, 296−300.
(24) Alam, T. M.; Childress, K. K.; Pastoor, K.; Rice, C. V. Characterization of Free, Restricted, and Entrapped Water Environments in Poly(N-isopropyl acrylamide) Hydrogels via H-1 HRMAS PFG NMR Spectroscopy. *J. Polym. Sci., Part B: Polym. Phys.* **2014**, *52*, 1521−1527.
(25) Kametani, S.; Sekine, S.; Ohkubo, T.; Hirano, T.; Ute, K.; Cheng, H. N.; Asakura, T. NMR studies of water dynamics during sol-to-gel transition of poly (N-isopropylacrylamide) in concentrated aqueous solution. *Polymer* **2017**, *109*, 287−296.
(26) Philipp, M.; Kyriakos, K.; Silvi, L.; Lohstroh, W.; Petry, W.; Krüger, J. K.; Papadakis, C. M.; Müller-Buschbaum, P. From Molecular Dehydration to Excess Volumes of Phase-Separating PNIPAM Solutions. *J. Phys. Chem. B* **2014**, *118*, 4253−4260.
(27) Niebuur, B.-J.; Lohstroh, W.; Appavou, M.-S.; Schulte, A.; Papadakis, C. M. Water Dynamics in a Concentrated Poly(N-isopropylacrylamide) Solution at Variable Pressure. *Macromolecules* **2019**, *52*, 1942−1954.
(28) Park, S.; Fayer, M. D. Hydrogen bond dynamics in aqueous NaBr solutions. *Proc. Natl. Acad. Sci. U. S. A.* **2007**, *104*, 16731−16738.
(29) Bakker, H. J. Structural Dynamics of Aqueous Salt Solutions. *Chem. Rev.* **2008**, *108*, 1456−1473.
(30) Giammanco, C. H.; Wong, D. B.; Fayer, M. D. Water Dynamics in Divalent and Monovalent Concentrated Salt Solutions. *J. Phys. Chem. B* **2012**, *116*, 13781−13792.
(31) Roget, S. A.; Carter-Fenk, K. A.; Fayer, M. D. Water Dynamics and Structure of Highly Concentrated LiCl Solutions Investigated Using Ultrafast Infrared Spectroscopy. *J. Am. Chem. Soc.* **2022**, *144*, 4233−4243.
(32) Rezus, Y. L. A.; Bakker, H. J. Effect of urea on the structural dynamics of water. *Proc. Natl. Acad. Sci. U. S. A.* **2006**, *103*, 18417.
(33) Rezus, Y. L. A.; Bakker, H. J. Observation of Immobilized Water Molecules around Hydrophobic Groups. *Phys. Rev. Lett.* **2007**, *99*, 148301−148314.
(34) Wong, D. B.; Sokolowsky, K. P.; El-Barghouthi, M. I.; Fenn, E. E.; Giammanco, C. H.; Sturlaugson, A. L.; Fayer, M. D. Water Dynamics in Water/DMSO Binary Mixtures. *J. Phys. Chem. B* **2012**, *116*, 5479−5490.
(35) Moilanen, D. E.; Fenn, E. E.; Wong, D.; Fayer, M. D. Water Dynamics in Large and Small Reverse Micelles: From Two Ensembles to Collective Behavior. *J. Chem. Phys.* **2009**, *131*, 014704.
(36) Fenn, E. E.; Wong, D. B.; Fayer, M. D. Water Dynamics at Neutral and Ionic Interfaces. *Proc. Natl. Acad. Sci. U. S. A.* **2009**, *106*, 15243−15248.
(37) Moilanen, D. E.; Fenn, E. E.; Wong, D.; Fayer, M. D. Water Dynamics in AOT Lamellar Structures and Reverse Micelles: Geometry and Length Scales vs. Surface Interactions. *J. Am. Chem. Soc.* **2009**, *131*, 8318−8328.
(38) Fenn, E. E.; Moilanen, D. E.; Levinger, N. E.; Fayer, M. D. Water Dynamics and Interactions in Water−Polyether Binary Mixtures. *J. Am. Chem. Soc.* **2009**, *131*, 5530−5539.
(39) Roget, S. A.; Kramer, P. L.; Thomaz, J. E.; Fayer, M. D. Bulk-like and Interfacial Water Dynamics in Nafion Fuel Cell Membranes Investigated with Ultrafast Nonlinear IR Spectroscopy. *J. Phys. Chem. B* **2019**, *123*, 9408−9417.
(40) Yan, C.; Kramer, P. L.; Yuan, R.; Fayer, M. D. Water Dynamics in Polyacrylamide Hydrogels. *J. Am. Chem. Soc.* **2018**, *140*, 9466−9477.
(41) Roget, S. A.; Piskulich, Z. A.; Thompson, W. H.; Fayer, M. D. Identical Water Dynamics in Acrylamide Hydrogels, Polymers, and Monomers in Solution: Ultrafast IR Spectroscopy and Molecular Dynamics Simulations. *J. Am. Chem. Soc.* **2021**, *143*, 14855−14868.
(42) Yamada, S. A.; Shin, J. Y.; Thompson, W. H.; Fayer, M. D. Water Dynamics in Nanoporous Silica: Ultrafast Vibrational Spectroscopy and Molecular Dynamics Simulations. *J. Phys. Chem. C* **2019**, *123*, 5790−5803.
(43) Fawcett, J. S.; Morris, C. J. O. R. Molecular-Sieve Chromatography of Proteins on Granulated Polyacrylamide Gels. *Sep. Sci.* **1966**, *1*, 9−26.
(44) Ogston, A. G. The spaces in a uniform random suspension of fibres. *Trans. Faraday Soc.* **1958**, *54*, 1754−1757.
(45) Xia, Y.; Yin, X.; Burke, N. A. D.; Stöver, H. D. H. Thermal Response of Narrow-Disperse Poly(N-isopropylacrylamide) Prepared by Atom Transfer Radical Polymerization. *Macromolecules* **2005**, *38*, 5937−5943.
(46) Corcelli, S.; Lawrence, C. P.; Skinner, J. L. Combined electronic structure/molecular dynamics approach for ultrafast infrared spectroscopy of dilute HOD in liquid H2O and D2O. *J. Chem. Phys.* **2004**, *120*, 8107−8117.
(47) Woutersen, S.; Bakker, H. J. Resonant intermolecular transfer of vibrational energy in liquid water. *Nature* **1999**, *402*, 507−509.
(48) Fenn, E. E.; Wong, D. B.; Fayer, M. D. Water Dynamics in Small Reverse Micelles in Two Solvents: Two-Dimensional Infrared Vibrational Echoes with Two-Dimensional Background Subtraction. *J. Chem. Phys.* **2011**, *134*, 054512.
(49) Steinel, T.; Asbury, J. B.; Zheng, J. R.; Fayer, M. D. Watching hydrogen bonds break: A transient absorption study of water. *J. Phys. Chem. A* **2004**, *108*, 10957−10964.
(50) Rezus, Y. L. A.; Bakker, H. J. On the orientational relaxation of HDO in liquid water. *J. Chem. Phys.* **2005**, *123*, 114502.

https://doi.org/10.1021/acs.jpcb.2c05506
J. Phys. Chem. B 2022, 126, 7066−7075

(51) Moilanen, D. E.; Fenn, E. E.; Wong, D.; Fayer, M. D. Water Dynamics at the Interface in AOT Reverse Micelles. *J. Phys. Chem. B* **2009**, *113*, 8560−8568.
(52) Moilanen, D. E.; Piletic, I. R.; Fayer, M. D. Water Dynamics in Nafion Fuel Cell Membranes: the Effects of Confinement and Structural Changes on the Hydrogen Bonding Network. *J. Phys. Chem. C* **2007**, *111*, 8884−8891.
(53) Corcelli, S.; Skinner, J. L. Infrared and Raman Line Shapes of Dilute HOD in Liquid H2O and D2O from 10 to 90 °C. *J. Phys. Chem. A* **2005**, *109*, 6154−6165.
(54) Moilanen, D. E.; Fenn, E. E.; Lin, Y. S.; Skinner, J. L.; Bagchi, B.; Fayer, M. D. Water inertial reorientation: Hydrogen bond strength and the angular potential. *Proc. Natl. Acad. Sci. U. S. A.* **2008**, *105*, 5295−5300.
(55) Petersen, C.; Tielrooij, K. J.; Bakker, H. J. Strong temperature dependence of water reorientation in hydrophobic hydration shells. *J. Chem. Phys.* **2009**, *130*, 214511.
(56) Nicodemus, R. A.; Corcelli, S. A.; Skinner, J. L.; Tokmakoff, A. Collective Hydrogen Bond Reorganization in Water Studied with Temperature-Dependent Ultrafast Infrared Spectroscopy. *J. Phys. Chem. B* **2011**, *115*, 5604−5616.
(57) Ortiz de Solorzano, I.; Bejagam, K. K.; An, Y.; Singh, S. K.; Deshmukh, S. A. Solvation dynamics of N-substituted acrylamide polymers and the importance for phase transition behavior. *Soft Matter* **2020**, *16*, 1582−1593.
(58) Tan, H.-S.; Piletic, I. R.; Riter, R. E.; Levinger, N. E.; Fayer, M. D. Dynamics of Water Confined on a Nanometer Length Scale in Reverse Micelles: Ultrafast Infrared Vibrational Echo Spectroscopy. *Phys. Rev. Lett.* **2005**, *94*, 057405.
(59) van der Post, S. T.; Bakker, H. J. The combined effect of cations and anions on the dynamics of water. *Phys. Chem. Chem. Phys.* **2012**, *14*, 6280−6288.
(60) Groot, C. C. M.; Bakker, H. J. A femtosecond mid-infrared study of the dynamics of water in aqueous sugar solutions. *Phys. Chem. Chem. Phys.* **2015**, *17*, 8449−8458.
(61) Kinosita, K.; Kawato, S.; Ikegami, A. A theory of fluorescence polarization decay in membranes. *Biophys. J.* **1977**, *20*, 289−305.
(62) Kinosita, K.; Ikegami, A.; Kawato, S. On the wobbling-in-cone analysis of fluorescence anisotropy decay. *Biophys. J.* **1982**, *37*, 461−464.
(63) Lipari, G.; Szabo, A. Effect of Librational Motion on Fluorescence Depolarization and Nuclear Magnetic-Resonance Relaxation in Macromolecules and Membranes. *Biophys. J.* **1980**, *30*, 489−506.
(64) Tan, H.-S.; Piletic, I. R.; Fayer, M. D. Orientational dynamics of water confined on a nanometer length scale in reverse micelles. *J. Chem. Phys.* **2005**, *122*, 174501.
(65) Laage, D.; Hynes, J. T. A Molecular Jump Mechanism of Water Reorientation. *Science* **2006**, *311*, 832−835.
(66) Laage, D.; Stirnemann, G.; Hynes, J. T. Why Water Reorientation Slows without Iceberg Formation around Hydrophobic Solutes. *J. Phys. Chem. B* **2009**, *113*, 2428−2435.
(67) Sterpone, F.; Stirnemann, G.; Hynes, J. T.; Laage, D. Water Hydrogen-Bond Dynamics around Amino Acids: The Key Role of Hydrophilic Hydrogen-Bond Acceptor Groups. *J. Phys. Chem. B* **2010**, *114*, 2083−2089.
(68) Laage, D.; Elsaesser, T.; Hynes, J. T. Water Dynamics in the Hydration Shells of Biomolecules. *Chem. Rev.* **2017**, *117*, 10694−10725.
(69) Tavagnacco, L.; Zaccarelli, E.; Chiessi, E. On the molecular origin of the cooperative coil-to-globule transition of poly(N-isopropylacrylamide) in water. *Phys. Chem. Chem. Phys.* **2018**, *20*, 9997−10010.

Recommended by ACS

The Two Phase Transitions of Hydrophobically End-Capped Poly(*N*-isopropylacrylamide)s in Water
Hao Ren, Françoise M. Winnik, *et al.*
JUNE 25, 2020
MACROMOLECULES
READ

Less-Ordered Hydration Shell around Poly(*N*,*N*-diethylacrylamide) Is Insensitive to the Clouding Transition
Di Zhou, Kenji Mochizuki, *et al.*
OCTOBER 20, 2021
THE JOURNAL OF PHYSICAL CHEMISTRY B
READ

Pressure Dependence of the Cononsolvency Effect in Aqueous Poly(*N*-isopropylacrylamide) Solutions: A SANS Study
Bart-Jan Niebuur, Christine M. Papadakis, *et al.*
MAY 05, 2020
MACROMOLECULES
READ

Temperature-Dependent Phase Behavior of the Thermoresponsive Polymer Poly(*N*-isopropylmethacrylamide) in an Aqueous Solution
Chia-Hsin Ko, Christine M. Papadakis, *et al.*
AUGUST 14, 2020
MACROMOLECULES
READ

Get More Suggestions >

https://doi.org/10.1021/acs.jpcb.2c05506
J. Phys. Chem. B 2022, 126, 7066−7075